INSTITUTE OF PHYSICS PUBLISHING JOURNAL OF PHYSICS: CONDENSED MATTER

J. Phys.: Condens. Matter **18** (2006) S783–S794 doi:10.1088/0953-8984/18/21/S06

Coherence of spin qubits in silicon

A M Tyryshkin[1], J J L Morton[2,3], S C Benjamin[2], A Ardavan[3], G A D Briggs[2], J W Ager[4] and S A Lyon[1]

[1] Department of Electrical Engineering, Princeton, NJ 08544, USA
[2] Department of Materials, Oxford University, Parks Road, Oxford OX1 3PH, UK
[3] The Clarendon Laboratory, Oxford University, Parks Road, Oxford OX1 3PU, UK
[4] Materials Sciences Division, Lawrence Berkeley National Laboratory, Berkeley, CA 94720, USA

E-mail: lyon@princeton.edu

Received 15 November 2005
Published 12 May 2006
Online at stacks.iop.org/JPhysCM/18/S783

Abstract

Given the effectiveness of semiconductor devices for classical computation one is naturally led to consider semiconductor systems for solid state quantum information processing. Semiconductors are particularly suitable where local control of electric fields and charge transport are required. Conventional semiconductor electronics is built upon these capabilities and has demonstrated scaling to large complicated arrays of interconnected devices. However, the requirements for a quantum computer are very different from those for classical computation, and it is not immediately obvious how best to build one in a semiconductor. One possible approach is to use spins as qubits: of nuclei, of electrons, or both in combination. Long qubit coherence times are a prerequisite for quantum computing, and in this paper we will discuss measurements of spin coherence in silicon. The results are encouraging—both electrons bound to donors and the donor nuclei exhibit low decoherence under the right circumstances. Doped silicon thus appears to pass the first test on the road to a quantum computer.

(Some figures in this article are in colour only in the electronic version)

1. Introduction

Semiconductor based qubits (quantum bits) and gates were among the earliest suggestions for physical realizations of quantum information processors [1–4]. Since those early proposals, numerous groups have tackled various aspects of the problem of defining and constructing quantum logic in a semiconductor. The popularity of semiconducting systems for quantum computers can be directly traced to their popularity for classical electronics. A huge base of knowledge and experience has been built up over the last half-century about all aspects of semiconductors—their electronic states, chemical purification, crystal growth, defect control, nanostructure fabrication, and so forth. Given their versatility, many different states inside a

semiconductor have been proposed as qubits. Some of these include excitons bound in quantum dots [1, 2, 5, 6], the spin of electrons trapped at donors or in quantum dots [4, 7–10], other low lying states of impurities [11], and nuclear spins of an either an impurity [3, 12] or the host semiconductor [13, 14], as well as combinations of one or more of these states.

In this paper we will limit ourselves to spin qubits, and consider both electrons and nuclei. Even with these limitations there are still numerous approaches to constructing the various quantum gates which are required for information processing. We will also limit ourselves to a single host semiconductor, silicon, because it is particularly well suited to obtaining long spin coherence. Among the common semiconductors, only the elemental ones (C, Si, and Ge) have stable isotopes without nuclear magnetic moments. The presence of unwanted magnetic moments can lead to decoherence of nuclear spins through spin diffusion. Such processes will also decohere the electron spins, as will motion of an electron through the random magnetic landscape of the nuclear moments. Recent work has demonstrated ways of mitigating some of the ill effects of the nuclear moments in other semiconductors [15, 16], but spin coherence times are not yet comparable to those in Si. Among the elemental semiconductors, germanium has a relatively strong spin–orbit interaction, while the spin–orbit effect for X-point electrons in silicon and diamond is unexpectedly weak [17]. Silicon device technology is much more advanced than that of diamond (though carbon nanomaterials such as fullerenes and nanotubes offer some unique possibilities), making it reasonably straightforward to envision quantum devices based upon well-known classical structures.

Shallow donors in silicon have many features which make them attractive candidates for spin qubits in a quantum computer [3, 7, 18–20]. The ground electronic state of the donors (except Li) is symmetrical and spin degenerate only, with a large gap (>10 meV) to the excited states, leading to exceptionally long electron spin relaxation times at liquid helium temperatures. The first measurements of electron spin relaxation for donors in silicon were done in late 1950s by Honig [21] and by Feher and Gere [22]. They found unusually long relaxation times (T_{1e}) which at first were assigned to nuclear relaxation processes [23] but later were confirmed to describe electron spin relaxation. Relaxation times $T_{1e} \sim 1$ h were measured at 1.25 K, limited by the direct one-phonon mechanism [24] when great care was taken to prevent exposure of the sample to light or room temperature radiation [22]. At higher temperatures (2–20 K) a two-phonon Orbach mechanism [25] begins to be important and the relaxation times drop sharply by many orders of magnitude to $\sim 10^{-6}$ s at 20 K [22, 26]. The transverse relaxation time was also found to be long, though considerably shorter than the longitudinal times; $T_{2e} = 240$ μs in natural silicon and $T_{2e} = 520$ μs in isotopically purified ^{28}Si [27, 28]. Recently it has been found that longer transverse times are possible: $T_{2e} = 60$ ms was determined at 7 K in isotopically purified ^{28}Si as will be discussed further below [29]. It is expected that T_{2e} will be longer at lower temperatures and with further isotopic purification of the ^{28}Si. Spin relaxation of the donor nuclei have been measured at high doping densities by nuclear magnetic resonance (NMR), but there is insufficient sensitivity to extend those measurements to much lower densities [30]. We will discuss recent measurements of the coupled system of electron and nuclear spins of a neutral ^{31}P donor in ^{28}Si using electron nuclear double-resonance (ENDOR) [31].

2. Experimental details

The silicon crystals used in these experiments were doped with phosphorus in the range 10^{15}–10^{16} P cm^{-3}. All other electrically active impurities had concentrations <mid-10^{14} cm^{-3}. Both natural silicon crystals (4.7% of ^{29}Si) and isotopically purified ^{28}Si, either bulk grown or as epitaxial layers 10–25 μm thick on p-type natural Si were used. The ^{28}Si-enriched material

contained a residual ^{29}Si concentration of ∼800 ppm as determined by secondary ion mass spectrometry [32, 33]. Pulsed EPR experiments were done using an X-band Bruker EPR spectrometer (Elexsys 580) equipped with a low temperature helium-flow cryostat (Oxford CF935). The temperature was controlled with a precision of better than 0.05 K using calibrated temperature sensors (Lakeshore Cernox CX-1050-SD) and an Oxford ITC503 temperature controller. This precision was needed because of the strong temperature dependence of the electron spin relaxation times (e.g., T_{1e} varies by 5 orders of magnitude between 7 and 20 K). The electron spin T_{2e} and T_{1e} were measured using 2-pulse electron spin echo (ESE) and inversion recovery experiments, respectively [34]. In the *bang–bang* decoupling experiment [35], a modified Davies ENDOR sequence was used with a second refocusing RF pulse added at the end of the pulse sequence [36]. Microwave pulses of duration 16 and 32 ns were used for $\pi/2$ and π rotations of the electron spin and RF pulses of 15–100 μs were used for π rotation of the ^{31}P nuclear spins.

3. Electron spin relaxation for shallow donors in silicon

3.1. Spin relaxation due to ^{29}Si nuclei in natural Si:P

Natural silicon contains 4.7% of ^{29}Si with nuclear spin, $I = 1/2$. Spins of two neighbouring ^{29}Si nuclei can flip-flop to exchange their polarization and by this dipole–dipole interaction the spin polarization can travel from one ^{29}Si site to another through the lattice, termed nuclear spin diffusion. An electron spin residing on a donor interacts with the surrounding ^{29}Si nuclei through the hyperfine interactions (contact and dipole) and therefore feels the ^{29}Si nuclear spin diffusion as fluctuations in the local magnetic field. This fluctuating nuclear field results in additional dephasing of the electron spin; a mechanism known as spectral diffusion.

The theory of nuclear-induced spectral diffusion was developed in 1960–70s [37–39] and more recently adapted to the exact wavefunctions and the lattice structure of P donors in silicon [40]. It results in non-exponential spin relaxation decays which can be described by $V(\tau) = V_0 \exp[-(2\tau/T_{SD})^n]$, where τ is the time between the two pulses of a Hahn echo experiment, T_{SD} is the characteristic time of spectral diffusion and n is an exponent stretching factor which may vary between 2 and 3 for different regimes of spectral diffusion [39]. Both T_{SD} and n are complicated functions of the nuclear spin concentration and the relative position of the flip-flopping nuclei with respect to each other and also of the flip-flopping pair with respect to the electron spin in the host lattice [40]. The breadth of the electron spin wavefunction and its magnitude on the surrounding nuclei is an important factor in determining the transition between different spectral diffusion regimes, e.g. from $n \sim 3$ to $n \sim 2$ [39].

To experimentally characterize the role of ^{29}Si-induced spectral diffusion in donor spin relaxation, we performed Hahn echo experiments using natural silicon with low P doping (8×10^{14} P cm^{-3}). At this low doping, the instantaneous diffusion effects (see next section) are not excessive and therefore the effect of nuclear spectral diffusion can be observed most cleanly. The measured echo decays (figure 1(A)) are non-exponential and are strongly dependent on the orientation of the applied magnetic field with respect to the crystal axes. The longest decay is found for the magnetic field oriented along [100] and the shortest decay for the field oriented along [111]. We fit these non-exponential decays using a function of the form:

$$V(\tau) = V_0 \exp[-2\tau/T_{2e} - (2\tau/T_{SD})^n], \tag{1}$$

where, in addition to the spectral diffusion term we include a second exponential time constant T_{2e} to account for other relaxation processes, including the T_{1e} related processes and instantaneous diffusion, both of which can be described by a simple exponential decay. In our

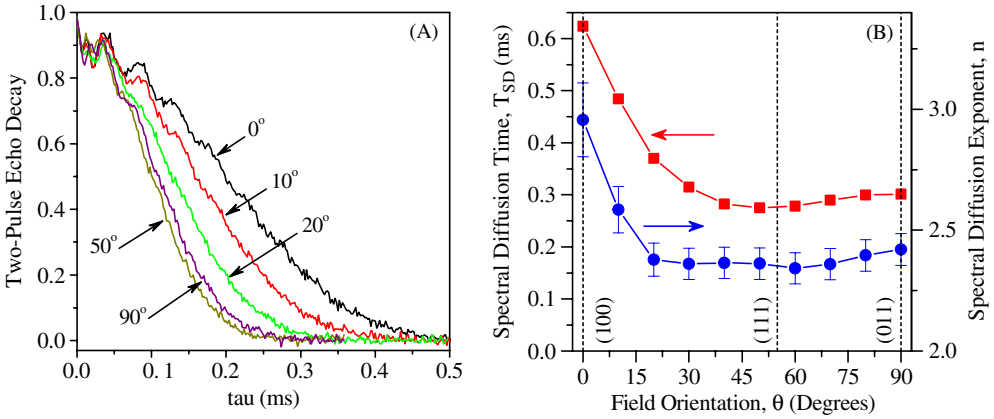

Figure 1. (A) The two-pulse echo decays in natural Si:P (8×10^{14} P cm^{-3}) at 8 K for selected orientations of the applied magnetic field B_0 with respect to the [100] crystal axis (field orientation is indicated with angle in degrees for each curve). The crystal rotation is done in the [100]–[011] plane. Weak oscillations superimposed on the decays at small τ are the electron spin echo envelope modulation caused by ^{29}Si. (B) The orientation dependence of the spectral diffusion time, T_{SD} (■, left axis) and the exponent, n (●, right axis) extracted from fitting the decay using equation (1). The vertical dashed lines indicate field orientations along specific axes of the silicon crystal.

fit we assumed T_{2e} to be orientation independent and the fit resulted in $T_{2e} = 1.1$ ms, mostly limited by instantaneous diffusion at this doping density. Both T_{SD} and n obtained from the fit show a strong orientation dependence (figure 1(B)), with T_{SD} changing from 0.62 ms for the field oriented along the [100]-direction to 0.27 ms along [111], and with n changing from 3 along [100] to 2.4 for the field tilted by $\theta \geqslant 20°$ from [100].

Gordon and Bowers noted that the echo decays were non-exponential [27] and Chiba and Hirai [28] have quantified these non-exponential decays for Si:P in echo experiments at a single field orientation along the [111]-direction. Their $T_{SD} = 0.36$ ms is in reasonable agreement with our data, however their $n = 3$ is noticeably different from our $n = 2.4$ along [111]. The non-exponential decays and similar orientation dependence for T_{SD} has also been reported by Abe *et al* [41] in natural silicon as well as in ^{29}Si-enriched silicon. However, they found an orientation independent n, and assumed $n \sim 2$ at all orientations in their analysis. For ^{29}Si-enriched silicon (∼99% ^{29}Si), they found T_{SD} to be about an order of magnitude shorter than in natural silicon, as would be expected because of faster spin diffusion in the ^{29}Si-rich media. In the next section we demonstrate that in ^{28}Si-purified silicon the non-exponential part in the echo decay is strongly suppressed and thus long purely exponential decays are observed (we estimate $T_{SD} > 8$ ms for 800 ppm of residual ^{29}Si in our ^{28}Si-purified silicon).

The orientation dependence for T_{SD} in silicon has recently been predicted theoretically by de Souza *et al* [40]. Their simulated decays were analysed in terms of a phase memory time, T_M, defined as the time for the echo signal decay to 1/e times its original magnitude. The stretch factor was calculated for a single orientation [111], where $n = 3$ was found. The trend in the predicted orientation dependence for T_M matches quite well with our T_{SD} dependence in figure 1(B), except for an overall scaling by a factor of 3.

3.2. Isotopically purified ^{28}Si:P

In very pure ^{28}Si silicon (800 ppm of residual ^{29}Si), the effect of nuclear spectral diffusion is small and therefore very long, exponential echo decays can be observed. While measuring

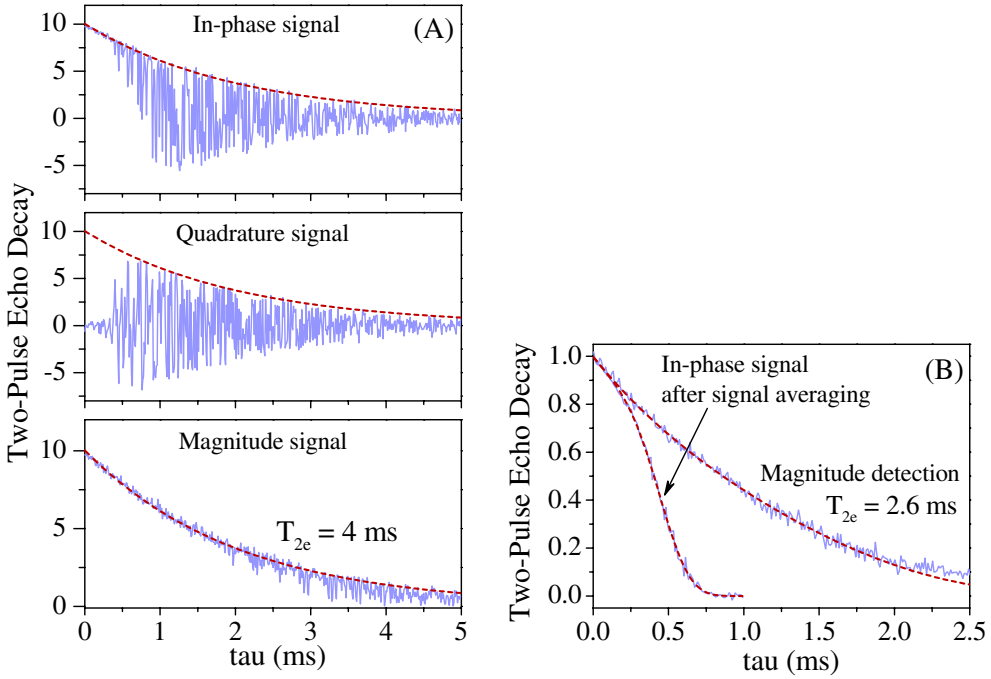

Figure 2. The 2-pulse echo decay for isotopically purified ^{28}Si:P crystal (5×10^{14} P cm^{-3}) at 8 K. (A) The in-phase (top) and quadrature (middle) signals measured in a single-shot experiment (e.g. no signal averaging). The fluctuations are nearly eliminated when the magnitude of the echo signal (bottom) is calculated as [in-phase^2 + quadrature^2]$^{1/2}$. The exponential fit to the magnitude signal in the bottom panel (red traces in each plot) corresponds to $T_{2e} = 4$ ms. (B) Signal averaging of the fluctuating in-phase signal results in a distorted, non-exponential echo decay approximated as $\exp[-2\tau/T_{2e} - (2\tau/T_{inst})^n]$, with $T_{inst} = 1.05$ ms and $n = 3.6$. Signal averaging of the magnitude signal reveals the much longer, exponential decay with $T_{2e} = 2.6$ ms for ^{28}Si:P (9×10^{14} P cm^{-3}) at 7 K.

long two-pulse echo decays we faced the problem of phase instability of the echo signal. This is illustrated in figure 2(A) where the as measured in-phase and quadrature signals of the microwave detector are shown in a single-shot experiment (e.g. without signal averaging). At long interpulse delays τ (>0.5 ms) strong 'noise' starts to develop and dominates the in-phase and quadrature signals. However, this noise largely disappears when the magnitude of the echo signal is calculated (bottom trace in figure 2(A)). Apparently the spins remain in phase with one another and form a strong echo signal at long τ, but they go out of phase with the spectrometer microwave source and therefore the echo signal fluctuates between the in-phase and quadrature detection channels. These phase fluctuations are caused by fluctuations in the magnetic field during the two-pulse echo experiment and possibly by fluctuations in the phase of the microwave source. We observed that characteristics of this instrumental noise vary significantly on different days and also depend upon various instrumental settings (orientation of the modulation coils with respect to the main magnetic field, settings in automatic frequency control circuit, etc).

Because of this instrumental phase noise, repetitive summation of the in-phase and quadrature echo signals (e.g. signal averaging to improve the signal-to-noise ratio) results in distorted echo decays with strongly non-exponential characteristics (figure 2(B)). To avoid these instrumental problems and to detect very long, undistorted echo decays we use single-shot detection. Instead of averaging the two detection channels separately and then obtaining

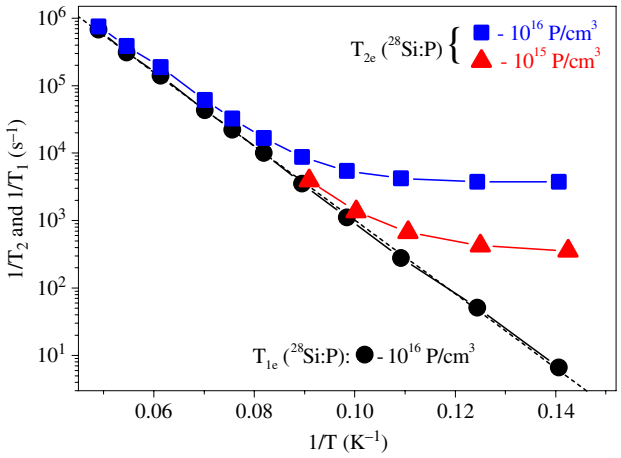

Figure 3. Temperature dependence of electron spin relaxation times, T_{1e} and T_{2e}, in isotopically purified ^{28}Si:P. The linear dependence of T_{1e} corresponds to the Orbach mechanism controlling the relaxation at this temperature range [26]. T_{2e} is controlled by the T_{1e} processes at high temperatures ($T > 10$ K) and by instantaneous diffusion at low temperatures [29].

the magnitude, we first calculate the magnitude signal, disregarding the fluctuating phase, and average this signal in repetitive experiments to improve the signal-to-noise ratio. This use of this magnitude detection approach requires that the signal is strong enough to be detected in a single-shot experiment. This requirement places a severe limit on two-pulse echo experiments, and only those samples with a spin concentration of about 10^{15} cm^{-3} or larger give sufficient signal for this procedure [29].

The T_{1e} and T_{2e} data and their temperature dependence in the range 7–20 K have been recently measured using pulsed ESR for isotopically purified ^{28}Si:P with 10^{15}–10^{16} P cm^{-3} [29]. In this temperature range T_{1e} is found to be independent of both the P concentration and the density of ^{29}Si. The Arrhenius plot (figure 3) shows that T_{1e} is controlled by an Orbach relaxation process with an energy gap to the first excited state, $\Delta E = 126$ K. This result is in good agreement with previous conclusions derived from continuous wave ESR measurements [26].

The temperature dependence of T_{2e} is more complex (figure 3). At high temperatures 12–20 K, T_{2e} closely follows the T_{1e} dependence, and thus T_{2e} is fully controlled by the T_{1e} relaxation processes in this temperature range. However, at lower temperature T_{2e} diverges from T_{1e}, and while T_{1e} continues to grow T_{2e} levels off and becomes temperature independent. The fact that the low temperature T_{2e} is approximately 10 times larger in the sample with a 10 times smaller P concentration suggests that at low temperatures T_{2e} is mostly determined by the dipole–dipole interactions between the donor electron spins.

One aspect of the dipole–dipole interaction between spins and its effect on a two-pulse echo experiment has been termed instantaneous diffusion [42]. The set of two-pulse echo decays shown in figure 4(A) was obtained using a variable rotation angle, θ_2, of the second microwave pulse. The relaxation time increases significantly at smaller rotation angles, and a very long $T_{2e} = 14$ ms is found at $\theta_2 = 45°$ as compared to $T_{2e} = 3.1$ ms at $\theta_2 = 170°$. This coherence time of 14 ms is the longest which has been directly measured for P donors in silicon. However, plotting the relaxation rate, $1/T_{2e}$, against $\sin^2(\theta_2/2)$ in figure 4(B) reveals a linear dependence with the slope proportional to the P donor concentration. By extrapolating to a very small θ_2 we are able to extract the $T_{2e} = 60(+50/-20)$ ms which corresponds to the

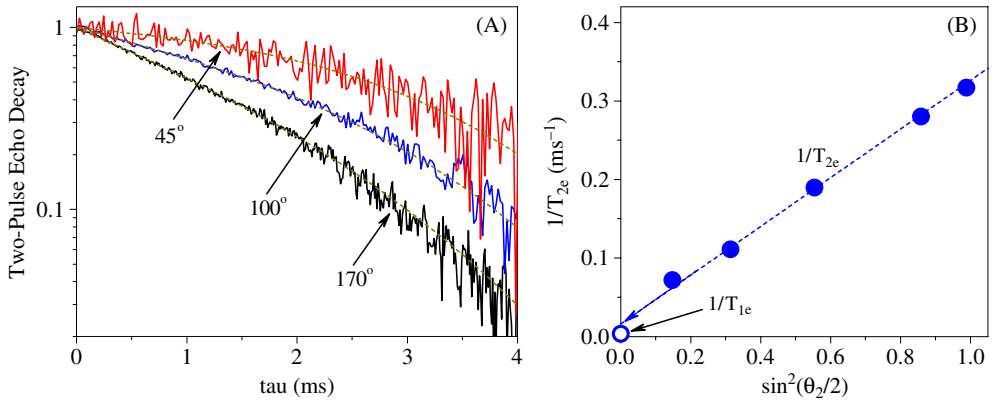

Figure 4. (A) The 2-pulse echo decays for isotopically purified ^{28}Si:P (9×10^{14} P cm^3) at 6.9 K and at different rotation angles θ_2 (indicated in degrees for each curve) of the second microwave pulse. The dashed lines are fits using $\exp[-2\tau/T_{2e} - (2\tau/T_{inst})^3]$, where the cubic term $T_{inst} \sim 8$ ms originates from incomplete phase noise cancellation and/or spectral diffusion from residual ^{29}Si (800 ppm). The fit to the echo decay curve with $\theta_2 = 45°$ gives $T_{2e} = 14$ ms. (B) A plot the relaxation rates $1/T_{2e}$ (●) as a function of the turning angle forms a line which extrapolates to $T_{2e} = 60$ ms at small θ_2. The point (○) corresponds to the measured $T_{1e} = 280$ ms at 6.9 K.

T_{2e} expected for an isolated donor in ^{28}Si. As also shown in figure 4(B), this extrapolated T_{2e} is similar to but somewhat shorter than T_{1e} measured for P donors at this temperature (6.9 K). Thus, T_{2e} of the isolated donor in ^{28}Si is probably limited by the T_{1e} relaxation processes down to at least 7 K.

4. Donor nuclear spins in Si:P

4.1. Coding spin qubits in silicon donors

All shallow donors in silicon (and their various isotopes) have non-zero nuclear spins and thus quite naturally, both the electron and nuclear spins of neutral donors have been proposed to be used for coding, manipulating and storing quantum information [3, 7, 18]. The ^{31}P donors are most popular choice among common donors because both the electron and nucleus have spin 1/2 and thus two qubits can be encoded using electron and nuclear spin states. The energy level diagram and qubit coding scheme are shown in figure 1(A). In the presence of a strong magnetic field the hyperfine coupling between the spins results in a non-uniform spacing of the energy levels and therefore selective excitation (or addressing) of the individual electron and nuclear spin transitions is possible by applying in-resonance microwave and radio frequency (RF) pulses. Single-qubit operations (spin rotations) are implemented by applying two pulses to coherently rotate two resolved electron (or nuclear) spin transitions. The two-qubit CNOT operation is even easier to perform since it requires only one RF pulse. The single-qubit gates and the two-qubit CNOT gate provide the universal set of gates and thus any other desired gates can be implemented [43].

4.2. Bang–bang decoupling of ^{31}P nuclear spin using controlled flips of electron spin

The ability to preserve quantum information coherently over an extended period of time is a prerequisite for a quantum system to be useful as qubit. As has been discussed above, the spin of electrons bound to donors have coherence times of at least $T_{2e} = 60$ ms at liquid helium temperatures which permits at least 10^6 single-qubit operations before the spin decoheres

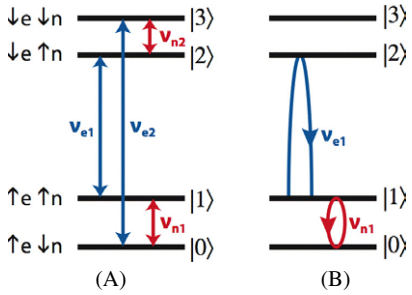

Figure 5. (A) An energy level diagram for the coupled electron–nuclear spin pair of neutral ^{31}P donor in silicon (electron spin $S = 1/2$, nuclear spin $I = 1/2$). In an applied magnetic field ($B_0 = 0.35$ T at X-band ESR), the transitions of the electrons are driven by microwave frequencies (ν_{e1}, ν_{e2}) near 10 GHz, while the nuclear spin transitions are driven by radio frequencies (ν_{n1}, ν_{n2}) at 50–60 MHz. The hyperfine coupling between the spins forces the spin energy levels to be spaced non-uniformly ($\nu_{e1} \neq \nu_{e2}$, and $\nu_{n1} \neq \nu_{n2}$) and therefore each of the allowed electron and nuclear transitions can be addressed individually with selective microwave and RF pulses, respectively. (B) In the *bang–bang* decoupling experiment a 2π rotation (ν_{e1}) is applied to the electron spin to produce a fast phase shift and thus to refocus the evolution of the nuclear spin driven by field ν_{n1} [35].

(we assume 60 ns long 2π pulses available in a standard pulsed ESR spectrometer). Although the relaxation times for donor nuclear spin have not been measured yet, it is anticipated that they are also very long, possibly in excess of the electron spin relaxation times. Longer relaxation times might be expected because of the smaller magnetic moment of the nuclei and thus weaker coupling to the fluctuating environment.

The concept of dynamical decoupling (DD), using a series of fast symmetrizing pulses to reduce (average out) the undesired parts of the system–environment interactions has been developed recently [44, 45]. If the DD scheme is introduced on top of the already long relaxation times in Si:P, the coherent evolution period of the system can be extended even further. Here we demonstrate one possible DD implementation for Si:P using the advantage of having two strongly coupled spins, electron and nuclear, in the donor. We implement a *bang–bang* decoupling pulse protocol to manipulate one (electron) spin in the coupled pair to effectively decouple the second (nuclear) spin from the decohering environment. This approach was first demonstrated for a similar system of coupled electron and nuclear spins ($S = 3/2$ and $I = 1$) in endohedral fullerenes, N@C$_{60}$ [35].

To demonstrate the full power of the *bang–bang* decoupling pulse scheme, we intentionally introduce a strong 'environmental' perturbation to the nuclear ^{31}P spin of the donor by applying a resonant RF field (ν_{n1}) to drive Rabi nutations between the nuclear spin states $|0\rangle$ and $|1\rangle$ (figure 5(B)). This strong RF field is then successfully decoupled by applying fast, selective 2π pulses (ν_{e1}) to rotate the electron spin around closed cycles between states $|1\rangle$ and $|2\rangle$. By mean of these selective ν_{e1} rotations, rapid 180° phase shifts are introduced to the nuclear spin state $|1\rangle$, while the phase of state $|0\rangle$ remains unchanged:

$$\Psi_i = a|0\rangle + b|1\rangle \xrightarrow{2\pi(\nu_{e1})} \Psi_f = a|0\rangle - b|1\rangle. \tag{2}$$

This phase shift can refocus the RF-driven evolution of the nuclear spin.

The experimental demonstration of this effect is shown in figure 6. The unperturbed Rabi nutation of the nuclear spin between the states $|0\rangle$ and $|1\rangle$ is driven by the long RF pulse (ν_{n1}) as shown in figure 6(A). The amplitude of the Rabi oscillations decreases as the RF pulse duration increases because the RF field inhomogeneity; spins in different part of the sample have slightly

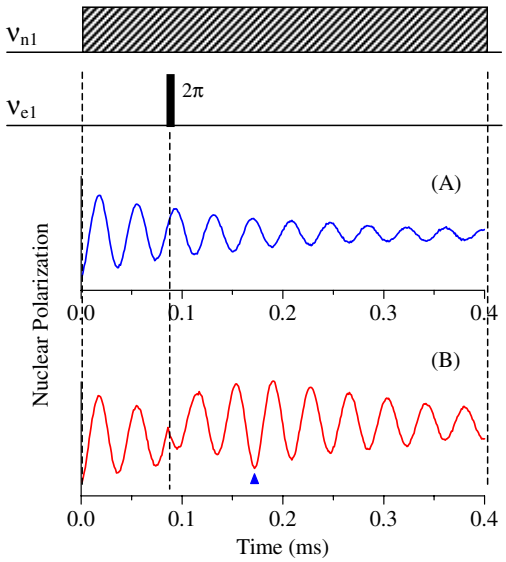

Figure 6. Rabi nutation of the ^{31}P nuclear spin of phosphorus donor in silicon driven by a long RF pulse at $\nu_{n1} = 52.33$ MHz. The timing diagram for the RF (ν_{n1}) and microwave (ν_{e1}) pulses used in the experiment is shown at top of the figure (the respective transitions are indicated in figure 1(B)). Free Rabi nutation in (A) is interrupted in (B) by applying a fast 2π rotation (ν_{e1}) to the electron spin at time 92 μs. This 2π rotation causes a nearly instantaneous phase shift to the nuclear spin and refocuses its evolution back to the initial state (indicated by ▲). The observed baseline shift after application the 2π pulse is the result of an imperfect 2π rotation of the electron spin.

different nutation frequency and gradually lose coherence at long times. Application of the 2π pulse to the donor electron spin at time $t_p = 92$ μs induces a nearly instantaneous (on the time scale of the nuclear nutation) phase shift to the nuclear spin nutation (figure 6(B)). The action of the RF field is reversed following this phase shift. After a further evolution period t_p (at the time indicated with ▲ in figure 6(B)) the nuclear spin nutation recovers its full amplitude indicating that all nuclear spins are in phase again and thus the decoherence caused by the inhomogeneity of the RF field is fully refocused at this point.

Figure 7 shows a logical extension to the above experiment [35]. By applying a series of the 2π pulses at a higher repetition rate than the nuclear nutation frequency, the nuclear spin evolution can be continuously refocused and thus locked in one particular state (figure 7(B)). It can then be released as desired to be locked again later in a different state upon application of a second series of the 2π pulses (figure 7(C)). These experiments demonstrate an unprecedented level of environmental decoupling (even against the strong in-resonance RF field artificially introduced in this experiment) which can be achieved using a relatively simple *bang–bang* pulse protocol. Our ability to implement this method for the donor in silicon is directly related to having two coupled (electron and nuclear) spins in the donor and the ability to selectively and independently rotate each allowed spin transition in the coupled system. This demonstrates the potential benefits of physical 'qubit' systems beyond the simple 2-level structure.

5. Conclusions

In this paper, we have reported our current progress in understanding spin relaxation for P donors in natural and ^{28}Si-purified silicon. In natural Si the spin relaxation is strongly affected by spectral diffusion due to presence of 4.7% ^{29}Si magnetic nuclei which decohere the electron

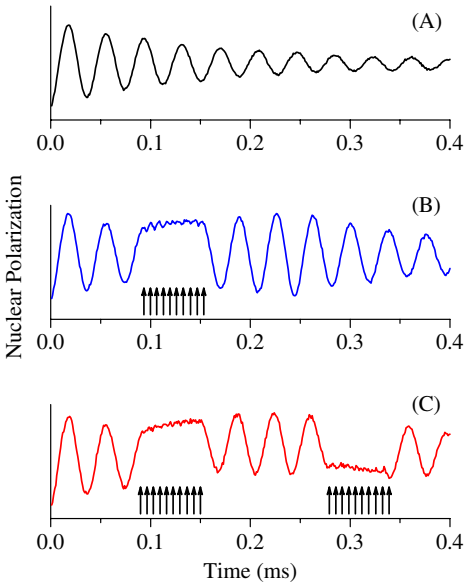

Figure 7. (A) Free Rabi nutation of the ^{31}P nuclear spin driven by a long RF pulse at ν_{n1} can be stopped at will and locked into a particular spin state (B) by applying a burst of the closely spaced 2π microwave pulses (ν_{e1}) to the electron spin. The position of the microwave pulses is schematically shown with vertical arrows. The nuclear spin nutation can then be released for further evolution to be locked later on in the opposite state (C) with a second burst of microwave pulses.

spin in less than 0.5 ms. Very long relaxation times (extrapolating to $T_{2e} = 60$ ms) have been found in isotopically pure ^{28}Si. We have also demonstrated that the spin states of both the electron and nucleus of a ^{31}P donor can be effectively controlled using resonant microwave and RF pulses. The *bang–bang* decoupling pulse protocol has been successfully implemented through the advantage of having coupled electron and nuclear spins in the donor. There are still many questions remaining to be answered. The implementation of two-qubit gates will require advanced processing, but the effects on spin coherence of this processing and of locating the spins in device structures is not yet known, for example. However, work on donor spins in silicon has established that this system can be considered a promising candidate for a future solid state quantum information processing technology.

Acknowledgments

We thank the Oxford–Princeton Link fund for support. Work at Princeton was supported by the ARO and ARDA under Contract No DAAD19-02-1-0040. The research at Oxford is part of the QIP IRC www.qipirc.org (GR/S82176/01). GADB thanks EPSRC for a Professorial Research Fellowship (GR/S15808/01). AA and SCB are supported by the Royal Society. JJLM is supported by St John's College, Oxford. Work at LBNL was supported by the Director, Office of Science, Office of Basic Energy Sciences, Materials Sciences and Engineering Division, of the US Department of Energy under Contract No DE-AC02-05CH11231.

References

[1] Lloyd S 1993 A potentially realizable quantum computer *Science* **261** 1569–71
[2] Ekert A and Jozsa R 1996 Quantum computation and Shor's factoring algorithm *Rev. Mod. Phys.* **68** 733–53

[3] Kane B E 1998 A silicon-based nuclear spin quantum computer *Nature* **393** 133–7
[4] Loss D and DiVincenzo D P 1998 Quantum computation with quantum dots *Phys. Rev.* A **57** 120–6
[5] Sherwin M S, Imamoglu A and Montroy T 1999 Quantum computation with quantum dots and terahertz cavity quantum electrodynamics *Phys. Rev.* A **60** 3508–14
[6] Bonadeo N H, Erland J, Gammon D, Park D, Katzer D S and Steel D G 1998 Coherent optical control of the quantum state of a single quantum dot *Science* **282** 1473–6
[7] Vrijen R, Yablonovitch E, Wang K, Jiang H W, Balandin A, Roychowdhury V, Mor T and DiVincenzo D 2000 Electron-spin-resonance transistors for quantum computing in silicon–germanium heterostructures *Phys. Rev.* A **62** 012306
[8] Imamoglu A, Awschalom D D, Burkard G, DiVincenzo D P, Loss D, Sherwin M and Small A 1999 Quantum information processing using quantum dot spins and cavity QED *Phys. Rev. Lett.* **83** 4204–7
[9] Dutt M V G, Cheng J, Li B, Xu X D, Li X Q, Berman P R, Steel D G, Bracker A S, Gammon D, Economou S E, Liu R B and Sham L J 2005 Stimulated and spontaneous optical generation of electron spin coherence in charged GaAs quantum dots *Phys. Rev. Lett.* **94** 227403
[10] Stoneham A M, Fisher A J and Greenland P T 2003 Optically driven silicon-based quantum gates with potential for high-temperature operation *J. Phys.: Condens. Matter* **15** L447–51
[11] Golding B and Dykman M I 2003 Acceptor-based silicon quantum computing *Preprint* cond-mat/0309147
[12] Skinner A J, Davenport M E and Kane B E 2003 Hydrogenic spin quantum computing in silicon: a digital approach *Phys. Rev. Lett.* **90** 087901
[13] Ladd T D, Goldman J R, Yamaguchi F, Yamamoto Y, Abe E and Itoh K M 2002 All-silicon quantum computer *Phys. Rev. Lett.* **89** 017901
[14] Taylor J M, Dur W, Zoller P, Yacoby A, Marcus C M and Lukin M D 2005 Solid-state circuit for spin entanglement generation and purification *Phys. Rev. Lett.* **94** 236803
[15] Koppens F H L, Folk J A, Elzerman J M, Hanson R, van Beveren L H W, Vink I T, Tranitz H P, Wegscheider W, Kouwenhoven L P and Vandersypen L M K 2005 Control and detection of singlet–triplet mixing in a random nuclear field *Science* **309** 1346–50
[16] Petta J R, Johnson A C, Taylor J M, Laird E A, Yacoby A, Lukin M D, Marcus C M, Hanson M P and Gossard A C 2005 Coherent manipulation of coupled electron spins in semiconductor quantum dots *Science* **309** 2180–4
[17] Liu L 1961 Valence spin–orbit splitting and conduction G tensor in Si *Phys. Rev. Lett.* **6** 683
[18] Kane B E 2000 Silicon-based quantum computation *Fortsch. Phys.-Prog. Phys.* **48** 1023–41
[19] Friesen M, Rugheimer P, Savage D E, Lagally M G, van der Weide D W, Joynt R and Eriksson M A 2003 Practical design and simulation of silicon-based quantum-dot qubits *Phys. Rev.* B **67** 121301
[20] Schenkel T, Persaud A, Park S J, Nilsson J, Bokor J, Liddle J A, Keller R, Schneider D H, Cheng D W and Humphries D E 2003 Solid state quantum computer development in silicon with single ion implantation *J. Appl. Phys.* **94** 7017–24
[21] Honig A and Combrisson J 1956 Paramagnetic resonance in As-doped silicon *Phys. Rev.* **102** 917–8
[22] Feher G and Gere E A 1959 Electron spin resonance experiments on donors in silicon. 2. Electron spin relaxation effects *Phys. Rev.* **114** 1245–56
[23] Honig A 1954 Polarization of arsenic nuclei in a silicon semiconductor *Phys. Rev.* **96** 234–5
[24] Van Vleck J H 1940 Paramagnetic relaxation times for titanium and chrome alum *Phys. Rev.* **57** 426
[25] Orbach R 1961 On theory of spin–lattice relaxation in paramagnetic salts *Proc. Phys. Soc. Lond.* **77** 821
[26] Castner T G 1962 Direct measurement of valley–orbit splitting of shallow donors in silicon *Phys. Rev. Lett.* **8** 13
[27] Gordon J P and Bowers K D 1958 Microwave spin echoes from donor electrons in silicon *Phys. Rev. Lett.* **1** 368–70
[28] Chiba M and Hirai A 1972 Electron-spin echo decay behaviors of phosphorus doped silicon *J. Phys. Soc. Japan* **33** 730
[29] Tyryshkin A M, Lyon S A, Astashkin A V and Raitsimring A M 2003 Electron spin relaxation times of phosphorus donors in silicon *Phys. Rev.* B **68** 193207
[30] Alloul H and Dellouve P 1987 Spin localization in Si:P—direct evidence from P-31 nuclear-magnetic-resonance *Phys. Rev. Lett.* **59** 578–81
[31] Feher G 1956 Observation of nuclear magnetic resonances via the electron spin resonance line *Phys. Rev.* **103** 834–5
[32] Ager J W, Beeman J W, Hansen W L, Haller E E, Sharp I D, Liao C, Yang A, Thewalt M L W and Riemann H 2005 High-purity, isotopically enriched bulk silicon *J. Electrochem. Soc.* **152** G448–51
[33] Itoh K M 2004 private communication
[34] Schweiger A and Jeschke G 2001 *Principles of Pulse Electron Paramagnetic Resonance* (Oxford: Oxford University Press)

[35] Morton J J L, Tyryshkin A M, Ardavan A, Benjamin S C, Porfyrakis K, Lyon S A and Briggs G A D 2006 Bang-bang control of fullerene qubits using ultra-fast phase gates *Nat. Phys.* **2** 40–3
[36] Tyryshkin A M, Lyon S A, Morton J J L and Davies A A 2005 ENDOR revisited: enhanced sensitivity and nuclear spin relaxation, in preparation
[37] Klauder J R and Anderson P W 1962 Spectral diffusion decay in spin resonance experiments *Phys. Rev.* **125** 912
[38] Zhidomirov G M and Salikhov K M 1969 Contribution to theory of spectral diffusion in magnetically diluted solids *Sov. Phys.—JETP* **29** 1037
[39] Milov A D, Salikhov K M and Tsvetkov Y D 1973 Phase relaxation of hydrogen-atoms stabilized in amorphous matrices *Fiz. Tverd. Tela* **15** 1187–95
[40] de Sousa R and Das Sarma S 2003 Theory of nuclear-induced spectral diffusion: spin decoherence of phosphorus donors in Si and GaAs quantum dots *Phys. Rev.* B **68** 115322
[41] Abe E, Itoh K M, Isoya J and Yamasaki S 2004 Electron-spin phase relaxation of phosphorus donors in nuclear-spin-enriched silicon *Phys. Rev.* B **70** 033204
[42] Salikhov K M, Dzuba S A and Raitsimring A M 1981 The theory of electron spin-echo signal decay resulting from dipole–dipole interactions between paramagnetic centers in solids *J. Magn. Reson.* **42** 255–76
[43] Divincenzo D P 1995 2-bit gates are universal for quantum computation *Phys. Rev.* A **51** 1015–22
[44] Viola L, Knill E and Lloyd S 1999 Dynamical decoupling of open quantum systems *Phys. Rev. Lett.* **82** 2417–21
[45] Zanardi P 1999 Symmetrizing evolutions *Phys. Lett.* A **258** 77–82